

Involvement of RNA granule proteins in meiotic silencing by unpaired DNA

Hua Xiao,[†] Michael M. Vierling,[†] Rana F. Kennedy, Erin C. Boone, Logan M. Decker, Victor T. Sy, Jackson B. Haynes, Michelle A. Williams,[‡] and Patrick K. T. Shiu*

Division of Biological Sciences, University of Missouri, Columbia, MO 65211, USA.

[†]These authors contributed equally to this work.

[‡]Present address: Department of Biology, McMaster University, Hamilton, ON L8S 4K1, Canada.

*Corresponding author: Division of Biological Sciences, University of Missouri, Columbia, MO 65211, USA. Email: shiup@missouri.edu

Abstract

In *Neurospora crassa*, expression from an unpaired gene is suppressed by a mechanism known as meiotic silencing by unpaired DNA (MSUD). MSUD utilizes common RNA interference (RNAi) factors to silence target mRNAs. Here, we report that *Neurospora* CAR-1 and CGH-1, homologs of two *Caenorhabditis elegans* RNA granule components, are involved in MSUD. These fungal proteins are found in the perinuclear region and P-bodies, much like their worm counterparts. They interact with components of the meiotic silencing complex (MSC), including the SMS-2 Argonaute. This is the first time MSUD has been linked to RNA granule proteins.

Keywords: meiotic silencing by unpaired DNA (MSUD); *Neurospora crassa*; P-bodies; RNA granules; RNA interference (RNAi)

Introduction

Neurospora crassa grows as an interconnected network of tubular cells (hyphae). Because the cross walls between individual cells are usually incomplete, viruses and transposons can potentially infiltrate the entire fungal colony. To defend against these invasive elements, *Neurospora* maintains several genome surveillance systems (Aramayo and Selker 2013; Gladyshev 2017). One example is known as meiotic silencing by unpaired DNA (MSUD), an RNA interference (RNAi) mechanism that targets unpaired genes for silencing during sexual development (Shiu et al. 2001; Hammond 2017). This process begins at meiotic prophase I, when a gene without a pairing partner is detected (presumably with the help of the SAD-6 homology search protein; Samarajeewa et al. 2014). A single-stranded aberrant RNA (aRNA) is then produced from the unpaired region and exported out of the nucleus. In the perinuclear region, the aRNA is processed by the meiotic silencing complex (MSC), which contains several RNAi-related proteins (Decker et al. 2015). The SAD-1 RNA-directed RNA polymerase (RdRP), with the help of the SAD-3 helicase, converts the aRNA into a double-stranded RNA (dsRNA; Shiu and Metzberg 2002; Hammond et al. 2011a). The DCL-1 Dicer cuts the dsRNA into small interfering RNAs (siRNAs), which are then made into single strands by the QIP exonuclease (Alexander et al. 2008; Xiao et al. 2010). The single-stranded siRNAs subsequently guide the SMS-2 Argonaute to target complementary mRNAs bound by nuclear cap-binding proteins NCBP1/2/3 (Lee et al. 2003; Decker et al. 2017; Boone et al. 2020). The SAD-2 scaffold protein functions to anchor many of the aforementioned factors to the perinuclear region

(Shiu et al. 2006; Decker et al. 2015). SAD-4 and SAD-5 are required for siRNA production, although their precise roles in the pathway are currently unclear (Hammond et al. 2013a, 2013b). Finally, SAD-7 may coordinate nuclear and extranuclear silencing events (Samarajeewa et al. 2017).

Made up of RNA-protein aggregates, processing bodies (P-bodies) are cytoplasmic granules associated with the regulation of RNA translation, storage, and degradation (Jain and Parker 2013; Corbet and Parker 2019). Although P-bodies are enriched in proteins involved in translation repression and mRNA decay, the exact role of these structures remains to be determined (Luo et al. 2018; Tibble et al. 2021). In mammals, it has been suggested that mRNA decay may not take place inside P-bodies (Standart and Weil 2018), i.e., P-bodies may function primarily to store mRNAs for later translation or decay (Riggs et al. 2020; Borbolis and Syntichaki 2021). In addition to the above, P-bodies have also been associated with RNAi (Jakymiw et al. 2007; Standart and Weil 2018). In this investigation, we explored the possibility that P-bodies are present during sexual development in *Neurospora* and asked whether some of their components are involved in MSUD.

Materials and methods

Fungal methods and genotypic information

Standard fungal protocols were followed throughout this study (<http://www.fgsc.net/Neurospora/NeurosporaProtocolGuide.htm>). Genotypes of *Neurospora* strains used are provided in Table 1.

Received: February 08, 2021. Accepted: May 13, 2021

© The Author(s) 2021. Published by Oxford University Press on behalf of Genetics Society of America.

This is an Open Access article distributed under the terms of the Creative Commons Attribution License (<http://creativecommons.org/licenses/by/4.0/>), which permits unrestricted reuse, distribution, and reproduction in any medium, provided the original work is properly cited.

Table 1 *Neurospora* strains used in this study

Strain	Genotype
F2-01	fl A (FGSC 4317)
F2-29	rid r ^Δ ::hph; fl A
F5-36	fl; sad-5 ^Δ ::hph a
F7-18	fl; cgh-1 ^Δ ::hph A
F8-01	car-1 ^Δ ::hph fl A
F8-10	rid; fl; mCherry-dcap-2::hph; mus-51 ^Δ ::bar A
F8-11	rid; fl; mCherry-dcap-2::hph; mus-51 ^Δ ::bar; sad-5 ^Δ ::hph A
F9-01	fl; mCherry-dcap-2::hph; mus-51 ^Δ ::bar; cgh-1 ^Δ ::hph a
P3-25	mep sad-1 ^Δ ::hph a
P9-42	Oak Ridge wild type (WT) a (FGSC 2490)
P11-67	cgh-1 ^Δ ::hph a
P17-70	r ^Δ ::hph; sad-5 ^Δ ::hph A
P24-40	rid; mCherry-dcap-2::hph; mus-51 ^Δ ::bar; gfp-cgh-1::hph A
P24-41	rid his-3; mCherry-dcap-2::hph; gfp-cgh-1::hph a
P24-42	rid; gfp-car-1::hph; mCherry-dcap-2::hph; mus-51 ^Δ ::bar A
P24-43	rid his-3; gfp-car-1::hph; mCherry-dcap-2::hph; mus-51 ^Δ ::bar a
P24-64	car-1 ^Δ ::hph a
P25-19	rid; gfp-car-1::hph; mCherry-cgh-1::nat A
P25-20	rid his-3; gfp-car-1::hph; mCherry-cgh-1::nat a
P25-21	rid; yfpc-car-1::hph; yfpc-cgh-1::nat A
P25-22	rid; yfpc-car-1::hph; yfpc-cgh-1::nat a
P25-27	rid; yfpc-car-1::hph; yfpc-sms-2::hph a
P25-28	rid; yfpc-car-1::hph A
P25-29	rid; yfpc-sms-2::hph yfpc-cgh-1::nat a
P25-30	rid; yfpc-sms-2::hph yfpc-cgh-1::nat A
P25-31	rid; yfpc-car-1::hph A
P25-32	rid; yfpc-car-1::hph; mus-51 ^Δ ::bar; yfpc-sad-2::hph a
P26-18	rid yfpc-sad-1::hph his-3; mus-51 ^Δ ::bar; yfpc-cgh-1::nat a
P26-19	rid yfpc-sad-1::hph; mus-51 ^Δ ::bar; yfpc-cgh-1::nat A
P26-20	rid his-3; mus-51 ^Δ ::bar yfpc-dcl-1::hph; yfpc-cgh-1::nat a
P26-21	rid; mus-51 ^Δ ::bar yfpc-dcl-1::hph; yfpc-cgh-1::nat A
P26-22	rid; yfpc-car-1::hph; mus-52 ^Δ ::bar; yfpc-dcl-1::nat a
P26-23	rid his-3; yfpc-car-1::hph; yfpc-dcl-1::nat A
P26-24	rid; yfpc-car-1::hph; yfpc-qip::nat mus-52 ^Δ ::bar a
P26-25	rid his-3; yfpc-car-1::hph; yfpc-qip::nat mus-52 ^Δ ::bar A
P26-26	rid yfpc-sad-1::nat; yfpc-car-1::hph a
P26-27	rid yfpc-sad-1::nat his-3; yfpc-car-1::hph A
P26-28	rid; mus-51 ^Δ ::bar; yfpc-sad-2::hph; yfpc-cgh-1::nat A
P26-29	rid; mus-51 ^Δ ::bar; yfpc-sad-2::hph; yfpc-cgh-1::nat a
P26-30	rid; yfpc-qip::hph; mus-51 ^Δ ::bar; yfpc-cgh-1::nat a
P26-31	rid; yfpc-qip::hph; mus-51 ^Δ ::bar; yfpc-cgh-1::nat A
P26-32	r ^Δ ::hph; cgh-1 ^Δ ::hph a
P26-34	r ^Δ ::hph; car-1 ^Δ ::hph a
P26-36	mCherry-dcap-2::hph a
P26-37	rid; mCherry-dcap-2::hph; mus-51 ^Δ ::bar; sad-5 ^Δ ::hph a
P27-18	car-1 ^Δ ::hph; mCherry-dcap-2::hph a
P27-19	rid; car-1 ^Δ ::hph; mCherry-dcap-2::hph; mus-51 ^Δ ::bar A
P27-20	rid; mCherry-dcap-2::hph; mus-51 ^Δ ::bar; cgh-1 ^Δ ::hph A

Genetic loci are described in the *Neurospora crassa* e-Compendium (http://www.bioinformatics.leeds.ac.uk/~gen6ar/newgenelist/genes/gene_list.htm).

Genetic markers and knockout mutants are originally from the Fungal Genetics Stock Center (FGSC; McCluskey et al. 2010) and the *Neurospora* Functional Genomics Group (Colot et al. 2006). Culturing and crossing media were prepared according to Vogel (1956) and Westergaard and Mitchell (1947), respectively.

Transcript analysis

For comparison of gene expression, *Neurospora* vegetative (SRR080688, SRR081479, SRR081546, and SRR081586) and sexual (SRR957218) RNA-seq datasets were obtained from the European Bioinformatics Institute (EBI)'s European Nucleotide Archive (ENA) (Ellison et al. 2011; Samarajeewa et al. 2014). Computational analysis of these datasets was performed as described (Decker et al. 2017).

Quantification of sexual spore production

fluffy (fl) strains were grown for six days in 24-well microplates (Corning #3524) at room temperature for use as designated females. Conidia (asexual spores) from each male strain were suspended in sterile water and adjusted to a concentration of 1000 counts/μl. For fertilization, 50 μl conidial suspension was inoculated on the female strain within a well. Ascospores (sexual spores) were collected from the lids 21 days post-fertilization and counted on a hemocytometer.

MSUD assays

Most assessments of MSUD proficiency were performed according to the method of Xiao et al. (2019), with crosses conducted in 24-well microplates and analyses based on shot ascospores. For cgh-1-null crosses, sexual development is too impaired for proficient spore shooting. Accordingly, spores from these crosses were extracted out of the fruiting bodies for progeny phenotyping.

Strain construction and confirmation

Green fluorescent protein (GFP) and mCherry tagging vectors were constructed using double-joint polymerase chain reaction (DJ-PCR; Hammond et al. 2011b; Samarajeewa et al. 2014). For strain confirmation, genomic DNA was isolated from conidia (Henderson et al. 2005) or vegetative hyphae (Qiagen DNeasy Plant Mini Kit). PCR-based validation of genotypes was conducted using the Promega GoTaq Green Master Mix or the Roche Expand Long Range dNTPack. When necessary, DNA sequencing was conducted by the University of Missouri (MU) DNA Core. Primers for strain construction and confirmation are listed in Supplementary Table S1.

Bimolecular fluorescence complementation

Bimolecular fluorescence complementation (BiFC) is an *in vivo* assay to detect protein-protein interaction. In BiFC, a functional fluorophore is restored when two halves of the yellow fluorescent protein (YFP) are brought together by the association of two interacting proteins (Hu et al. 2002; Bardiya et al. 2008). Tagging of YFP halves was performed as previously reported (Hammond et al. 2011b).

Photography and microscopy methods

Light microscopy images of protoperithecia (female structures), perithecia (fruiting bodies), and asci (spore sacs) were captured according to the methods of Decker et al. (2017). For fluorescent microscopy, a Leica TCS SP8 system was used. Preparation and visualization of asci were essentially as described (Alexander et al. 2008; Xiao et al. 2010).

Image analysis of P-bodies

Images of asci in the single-nucleus (diploid) stage were analyzed with Fiji v2.0.0-rc-69-1.52p (Schindelin et al. 2012). The mCherry-DCAP-2 signal was used as a marker for P-bodies. After using the "Set Scale" function to input the pixel/μm ratio for an image, the number and average size (area) of P-bodies were obtained with the "Analyze Particles" function. For each cross, 8–24 asci were analyzed. The P-values were calculated using the two-tailed Student's t-test.

Results

Presence of P-bodies in *Neurospora* meiotic cells

We asked if P-bodies are present during the sexual phase of *Neurospora*. The DCAP-2 decapping enzyme is often used as a

cellular marker for P-bodies (Sheth and Parker 2003; Gallo et al. 2008). Using mCherry-DCAP-2 (NCU07889), we have demonstrated that P-bodies can be seen in the asci (Figure 1B). To our knowledge, this is the first published P-body marker for *Neurospora*.

CAR-1 and CGH-1 localize in the perinuclear region and P-bodies

CAR-1 (Sm-domain protein) and CGH-1 (RNA helicase) family proteins are conserved P-body components (Jain and Parker, 2013). In *Caenorhabditis elegans*, they are also parts of germline P granules (Updike and Strome 2010; Sundby et al. 2021). We have identified the corresponding homologs in *Neurospora* (NCU03366 and NCU06149) and tagged them with GFP. As seen in Figure 1, A–H, CAR-1 and CGH-1 localize in both the perinuclear region and P-bodies. This is reminiscent of the observations in worms, in which CAR-1 and CGH-1 are found in both perinuclear P granules and cytoplasmic P-bodies (Updike and Strome 2010; Jain and Parker 2013; Ko et al. 2013).

CAR-1 and CGH-1 interact in P-bodies

CAR-1 and CGH-1 family proteins are known to have direct or indirect interaction with each other (Decker and Parker 2006; Roy

and Rajyaguru 2018). Because *Neurospora* CAR-1 and CGH-1 colocalize (Figure 1L), we tested whether they actually have physical association. Using BiFC, we have detected interaction between CAR-1 and CGH-1 in cytoplasmic P-bodies and not in the perinuclear region (Figure 2). It is possible that they do not interact in the perinuclear region at all or that their interaction there is indirect (e.g., through another protein).

Expression of *car-1* and *cgh-1* during both vegetative and sexual stages

To determine the expression profiles of *car-1* and *cgh-1*, we examined their transcript levels through RNA-seq datasets. While presumed MSUD-exclusive genes have relatively low vegetative expression (as compared to their sexual expression), *car-1* and *cgh-1* are abundantly expressed in both developmental stages (Table 2). These results hint that the two RNA granule proteins are probably active in both sexual and asexual cycles.

car-1^Δ and *cgh-1*^Δ mutants are slow growers

Deletion of the *car-1* or *cgh-1* homolog in yeast (*SCD6/DHH1*) is not lethal to the fungus (Hata et al. 1998; Kolesnikova et al. 2013). While *Neurospora car-1* and *cgh-1* are also nonessential, their losses are associated with slower linear growth (Figure 3A).

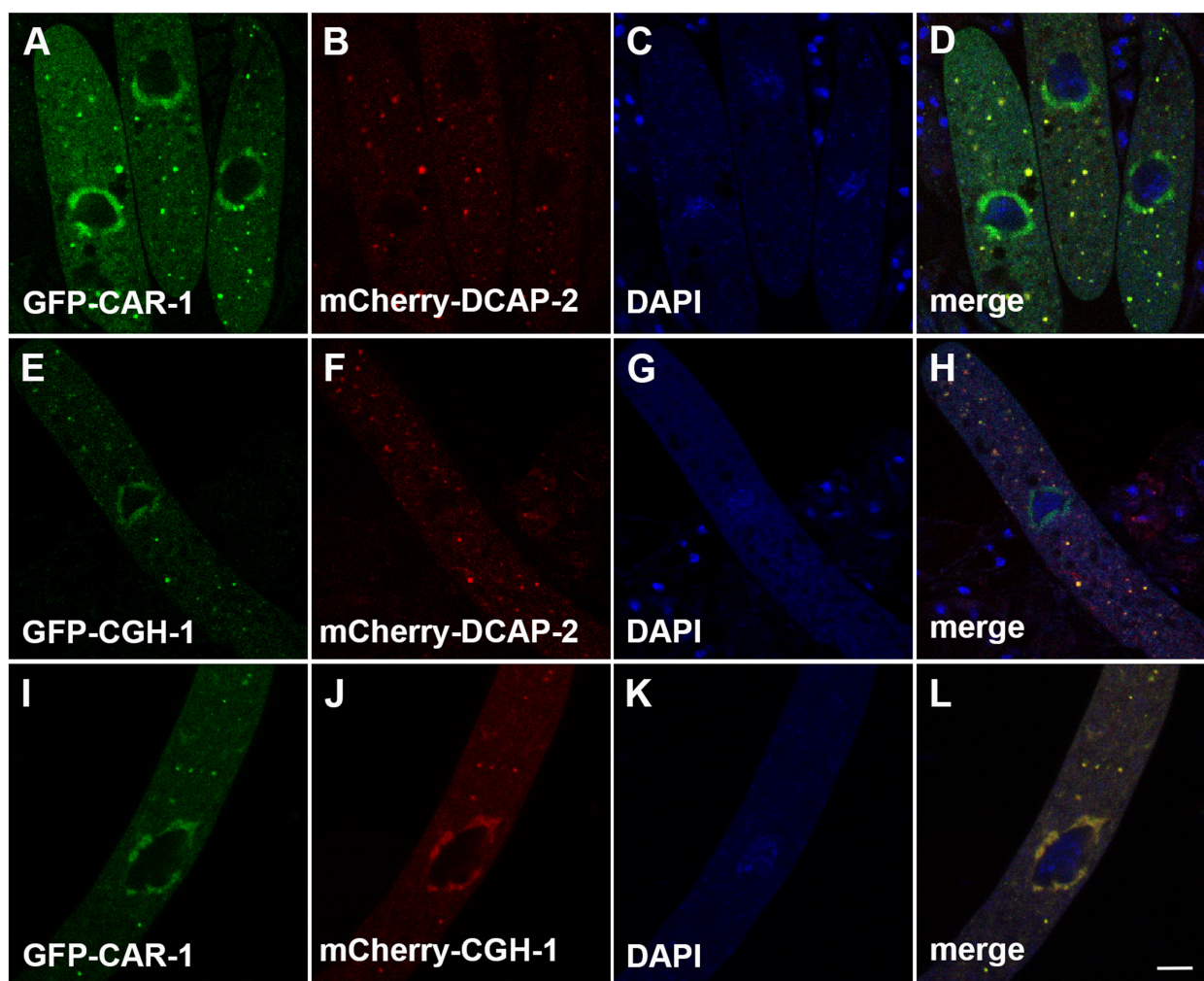


Figure 1 *Neurospora* CAR-1 and CGH-1 colocalize in the perinuclear region and P-bodies. DCAP-2 (decapping enzyme) is a P-body marker, and it colocalizes with cytoplasmic foci of CAR-1 and CGH-1 (D and H). Micrographs illustrate prophase asci expressing (A–D) *gfp-car-1* and *mCherry-dcap-2* (P24-42 × P24-43), (E–H) *gfp-cgh-1* and *mCherry-dcap-2* (P24-40 × P24-41), and (I–L) *gfp-car-1* and *mCherry-cgh-1* (P25-19 × P25-20). The chromatin was stained with DAPI. Bar, 5 μ m.

Interestingly, deletion of *cgh-1* leads to an abnormal conidiation pattern (Figure 3B), suggesting its possible involvement in asexual development.

Loss of CAR-1 or CGH-1 impairs sexual development

Because *car-1* and *cgh-1* are well expressed during sexual development, we asked if they are required for ascospore formation. Although crosses homozygous for *car-1^Δ* or *cgh-1^Δ* are not completely barren, they typically produce only 9 and 0.01% of the normal number of spores, respectively (Figure 4A). Examination of the mutant crosses showed that they are deficient in perithecial and ascus development (Figure 4B). These results demonstrate that normal sexual reproduction in *Neurospora* requires CAR-1 and CGH-1, similar to the case in worms (Audhya et al. 2005). In yeast, deletion of the *car-1* homolog (*DHH1*) also leads to severe mating defects (Ka et al. 2008).

CAR-1 and CGH-1 are important for MSUD

Because RNA granules are linked to post-transcriptional regulation (Anderson and Kedersha 2009; Tian et al. 2020), we asked whether CAR-1 and CGH-1 are important for MSUD in *Neurospora*. *Neurospora* normally produces American football-shaped spores. In an $r^+ \times r^Δ$ cross, the *round spore* gene is unpaired and silenced (Shiu et al. 2001), leading to the production of mostly round spores (or ~2–4% football; Figure 5, A and B). This “silenced”

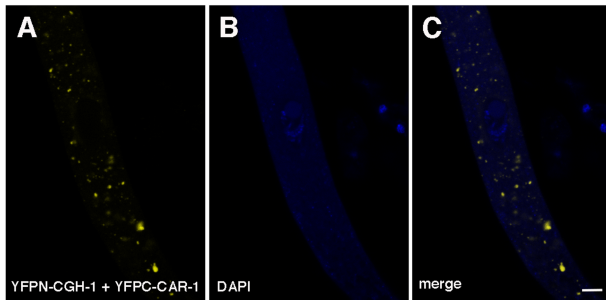


Figure 2 CAR-1 and CGH-1 interact in P-bodies. Interaction between tagged CAR-1 and CGH-1 allows the formation of a functional YFP (yellow) fluorophore. Micrographs illustrate prophase asci expressing *yfpn-cgh-1* and *yfpc-car-1* (P25-21 × P25-22). Bar, 5 μm.

Table 2 Expression of RNA silencing genes

Gene name	Gene no.	Vegetative expression (FPKM)	Sexual expression (FPKM)
RNA granules			
<i>car-1</i>	<i>ncu03366</i>	98.7509	65.0277
<i>cgh-1</i>	<i>ncu06149</i>	34.2955	72.2677
Housekeeping			
<i>actin</i>	<i>ncu04173</i>	2638.3425	905.4051
MSUD			
<i>sad-1</i>	<i>ncu02178</i>	0.3684	14.4495
<i>sad-2</i>	<i>ncu04294</i>	0.0000	38.5137
<i>sad-5</i>	<i>ncu06147</i>	0.0000	13.2559
<i>sms-2</i>	<i>ncu09434</i>	0.0496	673.0190
MSUD/Quelling			
<i>dcl-1</i>	<i>ncu08270</i>	4.4300	31.0978
<i>qip</i>	<i>ncu00076</i>	18.6841	107.2514

Quelling and MSUD refer to the vegetative and sexual silencing systems in *Neurospora*, respectively (Gladyshev 2017). FPKM, fragments per kilobase of exon per million mapped reads.

phenotype could be reversed (or partially reversed) by having an MSUD gene deletion in one or both parents (Hammond et al. 2013b). When one parent of an *r*-unpaired cross contains a *car-1^Δ* or *cgh-1^Δ* allele, 20 and 9% of the progeny are of football-shaped, respectively, suggesting that the two deletion mutations act as semidominant suppressors of MSUD (Figure 5A). In crosses homozygous for *car-1^Δ* or *cgh-1^Δ*, the figures go up to 63 and 81%, respectively (Figure 5B). These results suggest that the two RNA granule proteins are involved in the MSUD pathway.

CAR-1 and CGH-1 interact with components of the MSUD machinery

The perinuclear localization of CAR-1 and CGH-1 suggests that they could be linked to MSC, the silencing complex surrounding the nucleus. Indeed, as shown by BiFC, CAR-1 and CGH-1 interact with known MSC factors (*SAD-1*, *SAD-2*, *DCL-1*, *QIP*, and *SMS-2*; Figure 6). These interactions are consistent with the notion that CAR-1 and CGH-1 are involved (directly or indirectly) in the meiotic silencing of target mRNAs.

The absence of MSUD does not hinder visible P-body formation

In mammals, siRNA-mediated silencing induces P-body assembly (Lian et al. 2007). We asked if the absence of MSUD would diminish the production of visible P-bodies in *Neurospora* asci. *SAD-5* is crucial for the production of siRNAs, and MSUD becomes nonfunctional in its absence (Hammond et al. 2013b). As seen in Figure 7, the absence of *SAD-5* (and MSUD) does not reduce visible P-body formation (in terms of number and average size).

Because CAR-1 and CGH-1 are P-body factors (Jain and Parker 2013), we examined whether their absence would affect P-body formation in *Neurospora*. While the number of visible P-bodies is not obviously reduced in a cross devoid of *car-1* or *cgh-1*, their average size is (Figure 7).

Discussion

In this study, we have demonstrated the presence of P-bodies during sexual development in *Neurospora*. P-body formation could be a consequence of RNA silencing (Eulalio et al. 2007b). The silencing machinery could promote mRNA degradation and trigger

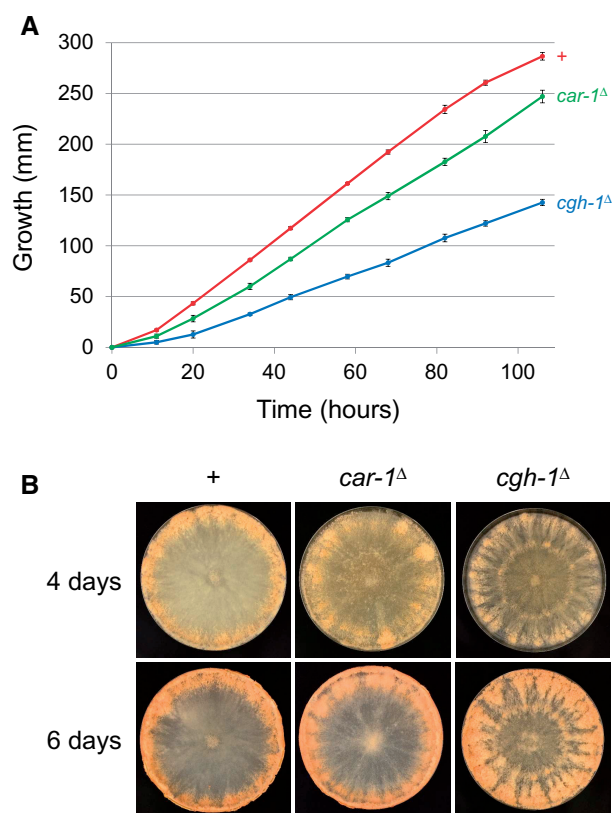


Figure 3 Vegetative phenotypes of *car-1* and *cgh-1* mutants. (A) Mutation in *car-1* (P24-64) or *cgh-1* (P11-67) leads to slower linear growth of the fungus, as compared to that of a + strain (P9-42). (B) For a *cgh-1* Δ strain, dense conidiation is not limited to the perimeter of an agar plate. +, wild type (WT) at pertinent loci.

the assembly of decay mRNA-protein complexes that aggregate into P-bodies (Anderson and Kedersha 2009). We did not observe a reduced P-body production in SAD-5's absence, which affects siRNA biogenesis during MSUD. If MSUD indeed involves P-bodies, one possibility is that visible P-body formation can be saturated by other pathways in MSUD's absence. Alternatively, MSUD may mainly involve submicroscopic ribonucleoprotein complexes (Leung and Sharp 2013). Aggregation into a visible entity may not confer additional advantages and is often not essential for RNA granule functions (Anderson and Kedersha 2009; Thomas et al. 2011; Leung and Sharp 2013).

CAR-1 and CGH-1 are involved in MSUD. The absence of either protein markedly reduces the severity of meiotic silencing. CAR-1 and CGH-1 are found in cytoplasmic P-bodies as well as the perinuclear region (the center of MSUD activity). The latter localization brings to mind the case in *C. elegans*, in which the two proteins are components of perinuclear P granules (germline structures important for post-transcriptional regulation; Sundby et al. 2021). The fact that RNA surveillance often happens in the perinuclear region is hardly a coincidence (also see examples in mammals and flies; Meikar et al. 2011; Kloc et al. 2014). It could provide an environment in which exported RNAs can meet up with their developmental regulators and have their fates effectively controlled (Voronina 2013; Decker et al. 2015).

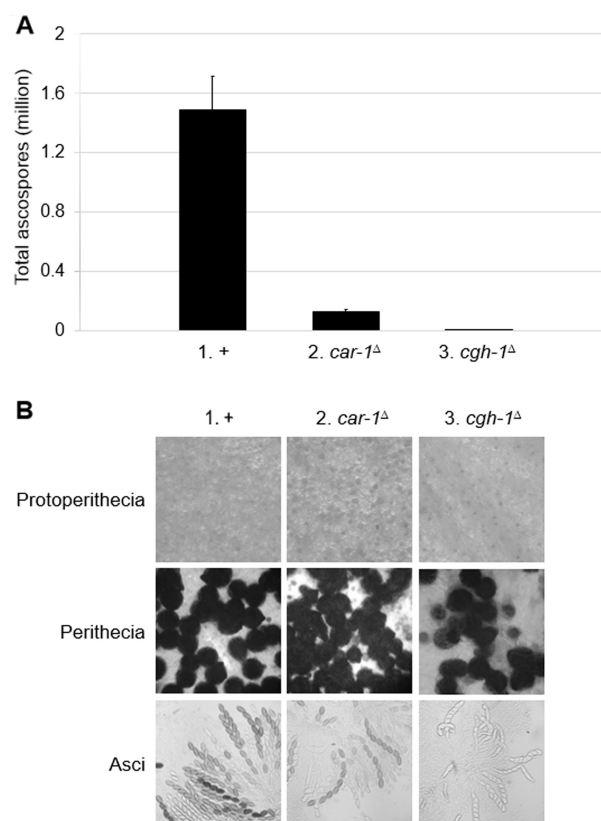


Figure 4 Crosses homozygous for *car-1* Δ or *cgh-1* Δ have defective sexual development. (A) Crosses missing *car-1* or *cgh-1* produce only a fraction of the spores seen in a normal cross (9 and 0.01%, respectively). (B) Although protoperithecial development appears proficient in *car-1* Δ and *cgh-1* Δ crosses, they only produce three-quarters and two-fifths of the normal number of mature perithecia, respectively. Dissected perithecia from these mutant crosses exhibit frequent and rampant ascus abortions. (1) F2-01 \times P9-42. (2) F8-01 \times P24-64. (3) F7-18 \times P11-67.

Using BiFC, we have shown that CGH-1 has interaction with the SMS-2 Argonaute. This is similar to the situation in human cells, in which a CGH-1 homolog (RCK) interacts with Argonaute proteins (to mediate translation repression; Chu and Rana 2006). It is possible that certain complex formations are conserved among different post-transcriptional networks. Interestingly, CAR-1 has also been shown to interact with the SMS-2 Argonaute in this study.

Although many components of the meiotic silencing machinery have been revealed, the final fates of MSUD-targeted mRNAs remain unclear. Our current model proposes that the SMS-2 Argonaute uses siRNAs to guide the slicing of complementary mRNAs (presumably in the perinuclear region). It is conceivable that targeted mRNA slicing is not 100% efficient and that unsliced (and possibly sliced) mRNAs are associated with certain RNA granule proteins for degradation, repression, and/or storage. CAR-1 and CGH-1 family proteins are presumed to be translation repressors and/or decapping activators (Eulalio et al. 2007a; Jain and Parker 2013; Zeidan et al. 2018). In the absence of CAR-1 or CGH-1, unsliced mRNAs could be inadvertently released for translation, allowing some expression of unpaired genes.

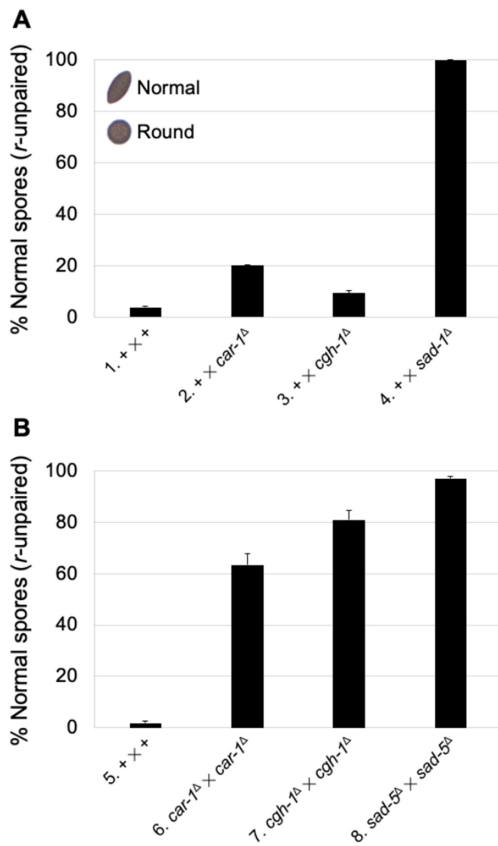


Figure 5 *car-1* and *cgh-1* are involved in MSUD. In *Neurospora*, a normal cross yields American football-shaped ascospores. Here, crosses heterozygous for *r*⁺ were tested. In an MSUD-proficient background, an unpaired *r*⁺ is silenced and nearly all of the progeny are round (with 2–4% football; crosses 1 and 5). (A) However, if one parent of an *r*-unpaired cross is *car-1*^Δ or *cgh-1*^Δ, the percentage of normal progeny goes up noticeably (with 20 and 9% football; crosses 2 and 3, respectively), suggesting that MSUD is impaired. (B) If both parents are *car-1*^Δ or *cgh-1*^Δ, progeny are predominantly normal (with 63 and 81% football; crosses 6 and 7, respectively). Also shown here are results for *sad-1*^Δ and *sad-5*^Δ (with 100 and 97% football; crosses 4 and 8, respectively), two standard MSUD suppressors used as positive controls (Hammond et al. 2013b). (1) F2-29 × P9-42. (2) F2-29 × P24-64. (3) F2-29 × P11-67. (4) F2-29 × P3-25. (5) F2-29 × P9-42. (6) F8-01 × P26-34. (7) F7-18 × P26-32. (8) F5-36 × P17-70.

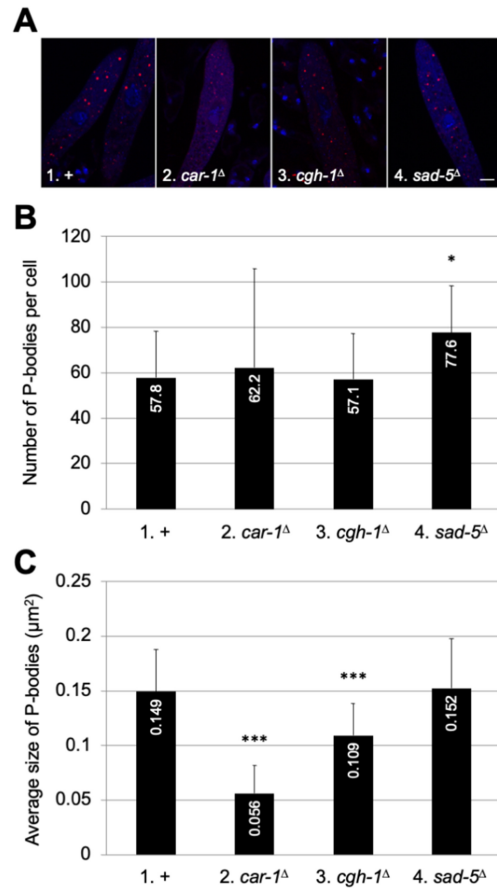


Figure 7 Visible P-body formation in various asci. (A) Micrographs illustrate prophase asci expressing *mCherry-dcap-2* in an MSUD-proficient cross (1, F8-10 × P26-36), a *car-1*-null cross (2, P27-18 × P27-19), a *cgh-1*-null cross (3, F9-01 × P27-20), and a *sad-5*-null cross (4, F8-11 × P26-37). Bar, 5 μm. (B) When compared to the control (+), none of the mutant crosses have a substantially lower P-body count. (C) The average size of P-bodies is markedly lower in a *car-1*^Δ or *cgh-1*^Δ background. For + versus mutant, * indicates *P* < 0.05 and *** indicates *P* < 0.001.

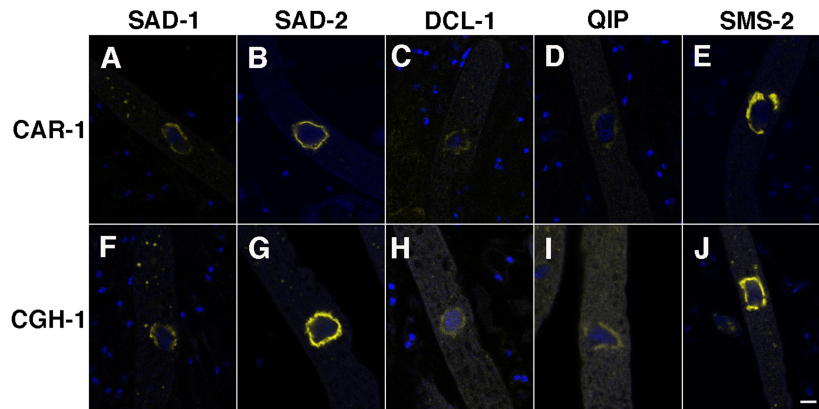


Figure 6 *CAR-1* and *CGH-1* interact with *SAD-1* (RdRP), *SAD-2* (scaffold protein), *DCL-1* (Dicer), *QIP* (exonuclease), and *SMS-2* (Argonaute). Micrographs illustrate prophase asci expressing (A) *yfpc-car-1* and *yfpn-sad-1* (P26-26 × P26-27), (B) *yfpc-car-1* and *yfpn-sad-2* (P25-31 × P25-32), (C) *yfpc-car-1* and *yfpn-dcl-1* (P26-22 × P26-23), (D) *yfpc-car-1* and *yfpn-qip* (P26-24 × P26-25), (E) *yfpc-car-1* and *yfpc-sms-2* (P25-27 × P25-28), (F) *yfpc-cgh-1* and *yfpc-sad-1* (P26-18 × P26-19), (G) *yfpc-cgh-1* and *yfpc-sad-2* (P26-28 × P26-29), (H) *yfpc-cgh-1* and *yfpc-dcl-1* (P26-20 × P26-21), (I) *yfpc-cgh-1* and *yfpc-qip* (P26-30 × P26-31), and (J) *yfpc-cgh-1* and *yfpc-sms-2* (P25-29 × P25-30). Bar, 5 μm.

Although the above hypothesis could explain our observations thus far, other possibilities abound. For example, CAR-1 and CGH-1 could enhance the activity of the SMS-2 Argonaute and/or other MSUD factors (i.e., their usual P-body functions are not involved in MSUD). Future work on these and other RNA granule components will shed light on how they regulate gene expression and diverse processes.

Data availability

Strains are available upon request. Supplementary material is available at figshare: <https://doi.org/10.25387/g3.14575689>.

Acknowledgments

We thank James Birchler and Patrice Albert for their equipment sharing and advice. We are indebted to the FGSC, the *Neurospora* Functional Genomics Group, the MU DNA/Molecular Cytology Core Facilities, colleagues from our community, and members of the Shiu Laboratory for their materials and help. We are pleased to acknowledge use of materials generated by P01 GM068087 “Functional Analysis of a Model Filamentous Fungus.”

Funding

R.F.K. and M.A.W. were supported by the MU Life Sciences Fellowship Program. E.C.B. was supported by a Graduate Assistance in Areas of National Need Fellowship from the U.S. Department of Education. L.M.D. was supported by a GK-12 Fellowship from the National Science Foundation (DGE1045322). V.T.S. was supported by an MU Arts and Science Career Development Scholarship. J.B.H. was supported by the MU Exposure to Research for Science Students (EXPRESS) Program. This work was supported by the MU Research Board, the MU Research Council, and the National Science Foundation (MCB1715534).

Conflicts of interest

None declared.

Literature cited

- Alexander WG, Raju NB, Xiao H, Hammond TM, Perdue TD, et al. 2008. DCL-1 colocalizes with other components of the MSUD machinery and is required for silencing. *Fungal Genet Biol.* 45:719–727.
- Anderson P, Kedersha N. 2009. RNA granules: post-transcriptional and epigenetic modulators of gene expression. *Nat Rev Mol Cell Biol.* 10:430–436.
- Aramayo R, Selker EU. 2013. *Neurospora crassa*, a model system for epigenetics research. *Cold Spring Harb Perspect Biol.* 5:a017921.
- Audhya A, Hyndman F, McLeod IX, Maddox AS, Yates JR, III, et al. 2005. A complex containing the Sm protein CAR-1 and the RNA helicase CGH-1 is required for embryonic cytokinesis in *Caenorhabditis elegans*. *J Cell Biol.* 171:267–279.
- Bardiya N, Alexander WG, Perdue TD, Barry EG, Metzberg RL, et al. 2008. Characterization of interactions between and among components of the meiotic silencing by unpaired DNA machinery in *Neurospora crassa* using bimolecular fluorescence complementation. *Genetics.* 178:593–596.
- Boone EC, Xiao H, Vierling MM, Decker LM, Sy VT, et al. 2020. An NCBP3-domain protein mediates meiotic silencing by unpaired DNA. *G3 (Bethesda).* 10:1919–1927.
- Borbolis F, Syntichaki P. 2021. Biological implications of decapping: beyond bulk mRNA decay. *FEBS J.* doi: 10.1111/febs.15798 (Preprint posted March 3, 2021).
- Chu CY, Rana TM. 2006. Translation repression in human cells by microRNA-induced gene silencing requires RCK/p54. *PLoS Biol.* 4:e210.
- Colot HV, Park G, Turner GE, Ringelberg C, Crew CM, et al. 2006. A high-throughput gene knockout procedure for *Neurospora* reveals functions for multiple transcription factors. *Proc Natl Acad Sci USA.* 103:10352–10357.
- Corbet GA, Parker R. 2019. RNP granule formation: lessons from P-Bodies and stress granules. *Cold Spring Harb Symp Quant Biol.* 84:203–215.
- Decker CJ, Parker R. 2006. CAR-1 and trailer hitch: driving mRNP granule function at the ER? *J Cell Biol.* 173:159–163.
- Decker LM, Boone EC, Xiao H, Shanker BS, Boone SF, et al. 2015. Complex formation of RNA silencing proteins in the perinuclear region of *Neurospora crassa*. *Genetics.* 199:1017–1021.
- Decker LM, Xiao H, Boone EC, Vierling MM, Shanker BS, et al. 2017. The nuclear cap-binding complex mediates meiotic silencing by unpaired DNA. *G3 (Bethesda).* 7:1149–1155.
- Ellison CE, Hall C, Kowbel D, Welch J, Brem RB, et al. 2011. Population genomics and local adaptation in wild isolates of a model microbial eukaryote. *Proc Natl Acad Sci USA.* 108:2831–2836.
- Eulalio A, Behm-Ansmant I, Izaurralde E. 2007a. P bodies: at the crossroads of post-transcriptional pathways. *Nat Rev Mol Cell Biol.* 8:9–22.
- Eulalio A, Behm-Ansmant I, Schweizer D, Izaurralde E. 2007b. P-body formation is a consequence, not the cause, of RNA-mediated gene silencing. *Mol Cell Biol.* 27:3970–3981.
- Gallo CM, Munro E, Rasoloson D, Merritt C, Seydoux G. 2008. Processing bodies and germ granules are distinct RNA granules that interact in *C. elegans* embryos. *Dev Biol.* 323:76–87.
- Gladyshev E. 2017. Repeat-induced point mutation and other genome defense mechanisms in fungi. *Microbiol Spectr.* 5:FUNK-0042-2017.
- Hammond TM. 2017. Sixteen years of meiotic silencing by unpaired DNA. *Adv Genet.* 97:1–42.
- Hammond TM, Xiao H, Boone EC, Perdue TD, Pukkila PJ, et al. 2011a. SAD-3, a putative helicase required for meiotic silencing by unpaired DNA, interacts with other components of the silencing machinery. *G3 (Bethesda).* 1:369–376.
- Hammond TM, Xiao H, Rehard DG, Boone EC, Perdue TD, et al. 2011b. Fluorescent and bimolecular-fluorescent protein tagging of genes at their native loci in *Neurospora crassa* using specialized double-joint PCR plasmids. *Fungal Genet Biol.* 48:866–873.
- Hammond TM, Spollen WG, Decker LM, Blake SM, Springer GK, et al. 2013a. Identification of small RNAs associated with meiotic silencing by unpaired DNA. *Genetics.* 194:279–284.
- Hammond TM, Xiao H, Boone EC, Decker LM, Lee SA, et al. 2013b. Novel proteins required for meiotic silencing by unpaired DNA and siRNA generation in *Neurospora crassa*. *Genetics.* 194:91–100.
- Hata H, Mitsui H, Liu H, Bai Y, Denis CL, et al. 1998. Dhh1p, a putative RNA helicase, associates with the general transcription factors Pop2p and Ccr4p from *Saccharomyces cerevisiae*. *Genetics.* 148:571–579.
- Henderson ST, Eariss GA, Catcheside DEA. 2005. Reliable PCR amplification from *Neurospora crassa* genomic DNA obtained from conidia. *Fungal Genet Newsl.* 52:24.

- Hu CD, Chinenov Y, Kerppola TK. 2002. Visualization of interactions among bZIP and Rel family proteins in living cells using bimolecular fluorescence complementation. *Mol Cell*. 9:789–798.
- Jain S, Parker R. 2013. The discovery and analysis of P Bodies. *Adv Exp Med Biol*. 768:23–43.
- Jakymiw A, Pauley KM, Li S, Ikeda K, Lian S, et al. 2007. The role of GW/P-bodies in RNA processing and silencing. *J Cell Sci*. 120:1317–1723.
- Ka M, Park YU, Kim J. 2008. The DEAD-box RNA helicase, Dhh1, functions in mating by regulating Ste12 translation in *Saccharomyces cerevisiae*. *Biochem Biophys Res Commun*. 367:680–686.
- Kloc M, Jedrzejowska I, Tworzydło W, Bilinski SM. 2014. Balbiani body, nuage and sponge bodies - The germ plasm pathway players. *Arthropod Struct Dev*. 43:341–348.
- Ko S, Kawasaki I, Shim YH. 2013. PAB-1, a *Caenorhabditis elegans* poly(A)-binding protein, regulates mRNA metabolism in germline by interacting with CGH-1 and CAR-1. *PLoS One*. 8:e84798.
- Kolesnikova O, Back R, Graille M, Séraphin B. 2013. Identification of the Rps28 binding motif from yeast Edc3 involved in the autoregulatory feedback loop controlling RPS28B mRNA decay. *Nucleic Acids Res*. 41:9514–9523.
- Lee DW, Pratt RJ, McLaughlin M, Aramayo R. 2003. An argonaute-like protein is required for meiotic silencing. *Genetics*. 164:821–828.
- Leung AK, Sharp PA. 2013. Quantifying Argonaute proteins in and out of GW/P-bodies: implications in microRNA activities. *Adv Exp Med Biol*. 768:165–182.
- Lian S, Fritzler MJ, Katz J, Hamazaki T, Terada N, et al. 2007. Small interfering RNA-mediated silencing induces target-dependent assembly of GW/P bodies. *Mol Biol Cell*. 18:3375–3387.
- Luo Y, Na Z, Slavoff SA. 2018. P-Bodies: composition, properties, and functions. *Biochemistry*. 57:2424–2431.
- McCluskey K, Wiest A, Plamann M. 2010. The Fungal Genetics Stock Center: a repository for 50 years of fungal genetics research. *J Biosci*. 35:119–126.
- Meikar O, Da Ros M, Korhonen H, Kotaja N. 2011. Chromatoid body and small RNAs in male germ cells. *Reproduction*. 142:195–209.
- Riggs CL, Kedersha N, Ivanov P, Anderson P. 2020. Mammalian stress granules and P bodies at a glance. *J Cell Sci*. 133:jcs242487.
- Roy D, Rajyaguru PI. 2018. Suppressor of clathrin deficiency (Scd6)—An emerging RGG-motif translation repressor. *WIREs RNA*. 9:e1479.
- Samarajeewa DA, Sauls PA, Sharp KJ, Smith ZJ, Xiao H, et al. 2014. Efficient detection of unpaired DNA requires a member of the rad54-like family of homologous recombination proteins. *Genetics*. 198:895–904.
- Samarajeewa DA, Manitchotpisit P, Henderson M, Xiao H, Rehard DG, et al. 2017. An RNA recognition motif-containing protein functions in meiotic silencing by unpaired DNA. *G3 (Bethesda)*. 7:2871–2882.
- Schindelin J, Arganda-Carreras I, Frise E, Kaynig V, Longair M, et al. 2012. Fiji: an open-source platform for biological-image analysis. *Nat Methods*. 9:676–682.
- Sheth U, Parker R. 2003. Decapping and decay of messenger RNA occur in cytoplasmic processing bodies. *Science*. 300:805–808.
- Shiu PKT, Metzberg RL. 2002. Meiotic silencing by unpaired DNA: properties, regulation, and suppression. *Genetics*. 161:1483–1495.
- Shiu PKT, Raju NB, Zickler D, Metzberg RL. 2001. Meiotic silencing by unpaired DNA. *Cell*. 107:905–916.
- Shiu PKT, Zickler D, Raju NB, Ruprich-Robert G, Metzberg RL. 2006. SAD-2 is required for meiotic silencing by unpaired DNA and perinuclear localization of SAD-1 RNA-directed RNA polymerase. *Proc Natl Acad Sci USA*. 103:2243–2248.
- Standart N, Weil D. 2018. P-Bodies: cytosolic droplets for coordinated mRNA storage. *Trends Genet*. 34:612–626.
- Sundby AE, Molnar RI, Claycomb JM. 2021. Connecting the dots: linking *Caenorhabditis elegans* small RNA pathways and germ granules. *Trends Cell Biol*. 31:387–401.
- Thomas MG, Loschi M, Desbats MA, Boccaccio GL. 2011. RNA granules: the good, the bad and the ugly. *Cell Signal*. 23:324–334.
- Tian S, Curnutte HA, Trcek T. 2020. RNA granules: a view from the RNA perspective. *Molecules*. 25:3130.
- Tibble RW, Depaix A, Kowalska J, Jemielity J, Gross JD. 2021. Biomolecular condensates amplify mRNA decapping by biasing enzyme conformation. *Nat Chem Biol*. 17:615–623.
- Updike D, Strome S. 2010. P granule assembly and function in *Caenorhabditis elegans* germ cells. *J Androl*. 31:53–60.
- Vogel HJ. 1956. A convenient growth medium for *Neurospora* (Medium N). *Microbial Genet Bull*. 13:42–43.
- Voronina E. 2013. The diverse functions of germline P-granules in *Caenorhabditis elegans*. *Mol Reprod Dev*. 80:624–631.
- Westergaard M, Mitchell HK. 1947. *Neurospora V*. A synthetic medium favoring sexual reproduction. *Am J Botany*. 34:573–577.
- Xiao H, Alexander WG, Hammond TM, Boone EC, Perdue TD, et al. 2010. QIP, an exonuclease that converts duplex siRNA into single strands, is required for meiotic silencing by unpaired DNA. *Genetics*. 186:119–126.
- Xiao H, Hammond TM, Shiu PKT. 2019. Suppressors of meiotic silencing by unpaired DNA. *Non-coding RNA*. 5:14.
- Zeidan Q, He F, Zhang F, Zhang H, Jacobson A, et al. 2018. Conserved mRNA-granule component Scd6 targets Dhh1 to repress translation initiation and activates Dcp2-mediated mRNA decay *in vivo*. *PLoS Genet*. 14:e1007806.

Communicating editor: R. B. Todd